

N 69 21 09 8  
NASA CR 100146

# CASE FILE COPY

DYNAMICS AND STABILITY OF FERROFLUIDS:

SURFACE INTERACTIONS

by

R. E. Zelazo and J. R. Melcher

CSR-TR-68-12

December, 1968

CENTER FOR SPACE RESEARCH  
MASSACHUSETTS INSTITUTE OF TECHNOLOGY



# DYNAMICS AND STABILITY OF FERROFLUIDS: SURFACE INTERACTIONS

by

Ronald E. Zelazo and James R. Melcher

Massachusetts Institute of Technology

Cambridge, Massachusetts

## Summary:

The nonlinear magnetization characteristics of recently developed ferrofluids complicate studies of wave dynamics and stability. A general formulation of the incompressible ferrohydrodynamics of a ferrofluid with nonlinear magnetization characteristics is presented which distinguishes clearly between effects of inhomogeneities in the fluid properties and saturation effects from nonuniform fields. The formulation makes it clear that with uniform and nonuniform fields the magnetic coupling with homogeneous fluids is confined to interfaces; hence it is a convenient representation for surface interactions.

Detailed attention is given to waves and instabilities on a planar interface between ferrofluids stressed by an arbitrarily directed magnetic field. The close connection with related work in electrohydrodynamics is cited and emphasis is given to the effect of the nonlinear magnetization characteristics on oscillation frequencies and conditions for instability. The effects of nonuniform fields are investigated using quasi-one-dimensional models for the imposed fields in which either a perpendicular or a tangential imposed field varies in a direction perpendicular to the interface. Three experiments are reported which support the theoretical models and emphasize the interfacial dynamics as well as the stabilizing effects of a tangential magnetic field. The resonance frequencies of ferrohydrodynamic surface waves are measured as a function of magnetization with fields imposed first

perpendicular, and second tangential, to the unperturbed interface. In a third experiment, the second configuration is augmented by a gradient in the imposed magnetic field to demonstrate the stabilization of a ferrofluid surface supported against gravity over air; the ferromagnetic stabilization of <sup>a</sup> Rayleigh-Taylor instability.

## I. Introduction

### A. Background

Ferrofluids, as recently developed by Rosensweig and his associates, are colloidal dispersions of sub-micron sized ferrite particles in a carrier or parent fluid such as kerosene (Rosenweig, 1966<sup>a</sup>). Unlike earlier fluids of this sort, the particles do not flocculate upon the application of strong magnetic fields; thermal agitation and the presence of a dispersing agent that coats each particle guarantee a permanent colloid. Experiments indicate that there is only a small dependence of viscosity and surface tension on magnetization. In kerosene-based fluids the conductivity, which is very small, is on the order of that of the base.

Numerous applications for these fluids appear possible, including novel energy conversion schemes (Resler and Rosensweig, 1967), levitation devices (Rosenweig, 1966<sup>b</sup>), and rotating seals (Rosenweig et al, 1968). In these developments, an understanding of the fundamental ferrofluid dynamics is essential.

Research has been carried forward to understand the static response of the fluids to the magnetization forces (Neuringer & Rosensweig, 1964). In systems of homogeneous ferrolíquids, surface interactions are particularly important, as emphasized by a recent investigation of the destabilizing influence of a magnetic field initially imposed normal to the flat interface of a ferrofluid (Cowley & Rosensweig, 1967). This work draws attention to the limitations arising from

static instability, and for the particular case considered, shows how account can be taken of nonlinear magnetization characteristics.

### B. Scope

In the work presented here, a general formulation is developed for studying wave dynamics and instability in nonlinear ferrofluids with bias fields that can not only have an arbitrary orientation, but can also be nonuniform. The formulation permits a clear distinction between the roles of inhomogeneity in the fluid properties and nonuniformities in the imposed magnetic field.

Consideration is given to interfacial dynamics and instability of homogeneous liquids separated by a planar interface stressed by a uniform field of arbitrary orientation. Then, the effects of field gradients in such systems are explored for particular field orientations. Finally, several experiments are described that serve to illustrate the nature of ferrofluid surface interactions, with emphasis given to the dynamic, rather than the static, behavior.

### C. Dielectrophoretic Analogy

If the magnetization characteristics of ferrofluids were linear, their dynamics would be the complete analog of electrohydrodynamic polarization interactions: dielectrophoretic phenomena (Pohl, 1960). Because much information is now available concerning this class of electrohydrodynamics, it is possible to cite a number of studies that have direct implications for ferrohydrodynamics. The analogy between dielectric and magnetic fluid mechanics is developed in <sup>an</sup>early work on linearly magnetized fluids (Melcher, 1963). The effects of free charge commonly mask dielectrophoretic effects, and so high frequency ac electric fields are often used to bias the fluids (Devitt & Melcher, 1965). Because of practical applications

to the orientation of cryogenic liquids in the zero-gravity environments of space, analyses have been made of systems of homogeneous and inhomogeneous liquids with interfaces stressed by essentially tangential fields with gradients directed perpendicular to their interfaces (Melcher & Hurwitz, 1967), of homogeneous liquids interacting with concentrated field gradients (Melcher et al, 1968), and of steady and dynamic linear and rotating flows confined by dielectrophoretic "walls" that take advantage of concentrated field gradients (Melcher et al, 1969) (Calvert & Melcher, 1969).

Much of the theoretical development which follows is motivated by this previous activity in electrohydrodynamics. The major contribution in placing this work in the context of ferrofluid dynamics is in the extensions of the formulation to the case of nonlinear magnetization characteristics. The theoretical extensions made here apply equally well to the dielectrophoretic interactions of liquids having nonlinear polarization characteristics.

## II. Formulation

### A. Magnetization and Deformation: Field Equations

In the class of magnetic liquids available, the magnetization density,  $\bar{M}$ , is induced colinear with the magnetic field intensity,  $\bar{H}$ . The magnetization magnitude characteristics of Fig. 1 therefore provide sufficient information for representing the effects of the fluid motion on the magnetic fields. In terms of the magnetic susceptibility,

$$\bar{M} = \chi(\alpha_1 \dots \alpha_n, H^2) \bar{H} \quad (1)$$

where  $H^2 = \bar{H} \cdot \bar{H}$ . Here, the parameters  $\alpha_1 \dots \alpha_n$  are local properties of the fluid. The susceptibility,  $\chi$ , is determined by this set of  $n$  parameters and the magnitude of the local magnetic field intensity. For example Eq. (1) might take

the forms (see Fig. 1)  $\chi = \alpha_1(\alpha_2 H^2 + 1)^{-1/2}$ , or  $\chi = \alpha_1 \operatorname{sech} \sqrt{H^2} \alpha_2$ , in which case there are only two  $\alpha_i$ 's. These might be determined by attempting to fit the assumed relation to the magnetization characteristic.

The characteristic (Fig. 1) represents the magnetization of a homogeneous liquid sample, a family of such curves is required to describe an inhomogeneous liquid. Although the parameter  $\alpha_i$  is similar to the parameter  $H^2$  in that it is an Eulerian function of space and time  $[\alpha_i(\bar{r}, t)]$ , it differs from  $H^2$  insofar as it represents the local magnetic properties of the fluid, and, ignoring effects of compressibility, can be identified with a given fluid particle. This results in

$$\frac{D\alpha_i}{Dt} = 0 \quad (2)$$

The dependences of the  $\alpha_i$ 's on  $\bar{r}$  account for the contribution of fluid inhomogeneity to variations in the local magnetization, while the dependence of  $H^2$  on  $\bar{r}$  accounts for the effect of a nonuniform magnetic field intensity.

It will be convenient at times to use the magnetic flux density  $\bar{B}$  and permeability  $\mu$ , where in the usual way

$$\bar{B} = \mu(\alpha_1, \dots, \alpha_n, H^2) \bar{H} ; \mu = \mu_0(\chi + 1) \quad (3)$$

MKS units are used, with  $\mu_0 = 4\pi \times 10^{-7}$ .

In writing the field equations for the stressed fluid, it is helpful to define the tensor

$$\zeta_{jk} = \frac{2}{\mu_0} H_j H_k \frac{\partial \mu}{\partial H^2} + \delta_{jk} \frac{\mu}{\mu_0} \quad (4)$$

where  $\delta_{jk}$  is the Kronecker delta function. If these parameters are evaluated at a given  $(\bar{M}, \bar{H})$  they can be written in terms of the appropriate susceptibilities  $\chi$  and  $\chi_s$  defined geometrically in terms of the M-H curve in Fig. 1. In terms of  $\chi$  and  $\chi_s$ , Eq. (4) becomes:



$$\zeta_{jk} = \frac{H_j H_k}{\bar{H} \cdot \bar{H}} (\chi_s - \chi) + \delta_{jk} (\chi + 1) \quad (5)$$

because  $\partial\mu/\partial H^2 = (\chi_s - \chi)\mu_o/2H^2$ .

Interest here centers around motions initiated from a static equilibrium wherein the magnetic field intensity has the equilibrium distribution  $\bar{H}^o(\bar{r})$ , and any inhomogeneity of the fluid is accounted for by equilibrium distributions of the  $\alpha_i$ 's,  $\alpha_i^o(\bar{r})$ . The dynamic field variables then take the form

$$\bar{H} = \bar{H}^o(\bar{r}) - \nabla\psi(\bar{r}, t) \quad (6)$$

$$\alpha_i = \alpha_i^o(\bar{r}) + \alpha_i'(\bar{r}, t) \quad (7)$$

where  $-\nabla\psi$  represents the perturbation magnetic field intensity and  $\alpha_i'$  the local perturbation in the magnetization parameter  $\alpha_i$ . Note that Eq. (6) automatically guarantees that perturbations in  $\bar{H}$  are irrotational. The condition that the magnetic flux density be solenoidal gives a relation that must be satisfied by  $\psi$  and the  $\alpha_i$ 's.

$$\nabla \cdot \left\{ [\mu^o(\bar{r}) + \mu'(\bar{r}, t)] [\bar{H}^o - \nabla\psi] \right\} = 0 \quad (8)$$

where the perturbation in permeability  $\mu'$  is, in turn:

$$\mu' = \sum_{i=1}^n \left( \frac{\partial \mu}{\partial \alpha_i} \right)^o \alpha_i' - 2 \left( \frac{\partial \mu}{\partial H^2} \right)^o \bar{H}^o \cdot \nabla\psi \quad (9)$$

with the superscript zero indicating quantities evaluated at  $[\alpha_i^o, (H^o)^2]$ .

To linear terms, these last two expressions require that  $\nabla \cdot \mu^o \bar{H}^o = 0$  and

$$\sum_{i=1}^n \nabla \cdot \left[ \bar{H}^o \left( \frac{\partial \mu}{\partial \alpha_i} \right)^o \alpha_i' \right] - \mu_o \frac{\partial}{\partial x_j} \left( \zeta_{jk}^o \frac{\partial \psi}{\partial x_k} \right) = 0 \quad (10)$$

with the components of  $\zeta_{jk}^o$  given by either Eq. (4) or Eq. (5) evaluated at  $[\alpha_i^o, (H^o)^2]$ . Terms where an index appears twice and the summation is not

indicated explicitly, are to be summed 1 to 3.

The linearization of Eq. (2) yields n additional equations which relate the  $\alpha_i$ 's to the velocity  $\bar{v}$  of the fluid.

$$\frac{\partial \alpha_i}{\partial t} + \bar{v} \cdot \nabla \alpha_i = 0 \quad (11)$$

These last two expressions embody the influence of the fluid motions on the magnetic field distribution.

### B. Force Density and Stress Tensor

For a linear relationship between M and H, where  $\chi$  and  $\mu$  are independent of  $H^2$ , the classic Korteweg-Helmholtz force density  $-H^2 \nabla \mu / 2$  and its associated stress tensor  $T_{ij} = \mu H_i H_j - \frac{1}{2} \delta_{ij} \mu H^2$  account for the coupling of the magnetic field to the fluid (Stratton, 1941). Because effects of magnetization in the absence of an applied field and thermodynamic effects such as fluid compressibility and temperature are considered insignificant for the present purposes, a derivation of the appropriate force density including the nonlinear magnetization can be made by considering conservation of energy for a thermodynamic subsystem consisting only of the magnetic fields as they are influenced by the geometric deformations of the magnetized fluids. Energy storage in kinetic form or in the form of internal (heat) energy is excluded. The basic conservation theorem for the subsystem states that inputs of electrical power either lead to an increase in energy stored in the magnetic field, or to work done on the mechanical environment through deformations of the fluid caused by the desired magnetization force density. This approach, so widely used in elementary lumped parameter electromechanics for finding total electrical forces (Woodson & Melcher, 1968<sup>a</sup>), has been used to find the magnetization force density for cases in which the M-H curves are linear (Woodson and Melcher, 1968<sup>b</sup>). Because the derivation



for the nonlinear case follows the same steps as given in this last reference, only a sketch of the more general derivation need be given here.

It is convenient to think of the fluid as being magnetized by a magnetic circuit having the excitation current  $i$ , with variations of continuum variables indicated by  $\delta( )$ . Thus, incremental variations in fluid displacements  $\bar{\xi}$  are given by  $\delta\bar{\xi}$ . Then, with the magnetic fields established and the excitation current,  $i$ , held constant, it can be shown that

$$\int_V [\delta w' - \bar{F} \cdot \delta\bar{\xi}] dV = 0 \quad (12)$$

with  $w'$  the coenergy density

$$w' = \int_0^{H^2} \frac{1}{2} \mu(\alpha_1 \dots \alpha_n, H^2) \delta H^2 \quad (13)$$

This latter expression is determined from the magnetization characteristic by establishing the current,  $i$ , with the fluid constrained mechanically.

The integration of Eq. (12) is carried out over the volume occupied by the magnetic field, and  $\bar{F}$  is the desired magnetization force density. The steps leading to this statement of conservation of energy are the same as for the case where  $M$  and  $H$  are linearly related. It can also be shown that because  $i$  is maintained constant

$$\int_V \delta w' dV = \int_V \sum_{i=1}^n \frac{\partial w'}{\partial \alpha_i} \delta \alpha_i dV \quad (14)$$

Then, because the  $\alpha_i$ 's are properties attached to the fluid particles,

$$\delta \alpha_i = - \delta \bar{\xi} \cdot \nabla \alpha_i \quad (15)$$

In view of the last two equations, conservation of energy, as expressed by Eq. (12), requires

$$\int_V \left[ -\frac{\partial w'}{\partial \alpha_i} \nabla \alpha_i - \bar{F} \right] \cdot \delta \bar{\xi} dV = 0 \quad (16)$$

In a treatment such as this,  $\bar{\xi}$  is a thermodynamically independent variable. Insofar as the isolated thermodynamic subsystem is concerned,  $\delta \bar{\xi}$  can be independently specified. Thus it follows that, although the volume,  $V$ , of Eq. (16) is not arbitrary (it includes all of the volume occupied by the magnetic field), because  $\delta \bar{\xi}$  is arbitrary the integrand must vanish, and therefore

$$\bar{F} = - \sum_{i=1}^n \frac{\partial w'}{\partial \alpha_i} \nabla \alpha_i \quad (17)$$

Because  $\bar{F}$  is defined in an incompressible fluid only to within the gradient of a pressure, there are other forms in which the force density can be correctly written (Cowley & Rosensweig, 1967; Penfield & Haus, 1967). This one is most convenient for the present purposes, because in systems of homogeneous fluids,  $\nabla \alpha_i = 0$ , except at interfaces. Thus, with  $\bar{F}$  in the form of Eq. (17), it is clear that the coupling is confined <sup>to interfaces</sup> for systems of homogeneous fluids in uniform and nonuniform fields. Furthermore, the surface force density caused by discontinuities in the  $\alpha_i$ 's is clearly perpendicular to the interface. As in the linear case, there are no shear surface force densities produced at interfaces by the magnetic field.

It is a matter of direct evaluation to show that Eq. (17) for the force density can be expressed in the form

$$\bar{F} = \nabla \cdot \bar{\bar{T}} ; \quad T_{ij} = \mu H_i H_j - \delta_{ij} w' \quad (18)$$

It is the components of  $\bar{\bar{T}}$  that will be used to write the interfacial force balance in Secs. III and IV.

### C. Equations of Motion

In addition to Eqs. (10) and (11), which represent the influence of fluid motion on the magnetic field distribution, and a linearized form of Eq. (17) or (18), a complete description of the fluid dynamics in magnetic fields requires the usual linearized Navier-Stokes equation for an inviscid fluid

$$\rho^0 \frac{\partial \bar{\mathbf{v}}}{\partial t} + \nabla(p^0 + p') = (\rho^0 + \rho') \bar{\mathbf{g}} + \bar{\mathbf{F}} \quad (19)$$

and conservation of mass for an incompressible fluid

$$\nabla \cdot \bar{\mathbf{v}} = 0 \quad (20)$$

$$\frac{\partial p'}{\partial t} + \bar{\mathbf{v}} \cdot \nabla \rho^0 = 0 \quad (21)$$

These equations represent  $3 + n$  scalar equations and one vector equation for the dependent variables  $\psi, p', \rho', \alpha_1, \dots, \alpha_n, \bar{\mathbf{v}}$

### III. Systems of Homogeneous Liquids: Uniform Fields

The fluid-field configuration shown in Fig. 2 is the basis for gaining considerable insight into the "self-field" dynamics of systems of ferrofluids. In regions (a) and (b), the fluid has uniform properties:  $\alpha_i^0 = \text{constant}$ . It follows from Eqs. (11) and (7) that the perturbations  $\alpha_i'$  are then zero. Then, as is evident from Eq. (17) for the force density, coupling is confined to the interface. To make matters even simpler, an exact solution for the equilibrium magnetic field in each region, as generated by the surface currents and the magnet poles, is  $\bar{\mathbf{H}}^0 = H_x^0 \bar{\mathbf{i}}_x + H_y^0 \bar{\mathbf{i}}_y$ , where in a given region individual components are uniform. Thus, the parameters  $\zeta_{ij}^0$  are constants in a given region, determined by the properties of the appropriate fluid and the relative magnitudes of the field components. If the equilibrium quantities are to be associated with a given fluid, the superscript (o) is replaced by an (a) or (b).

In the following sections the dispersion equation is developed for waves on the interface. Because the imposed fields are uniform, the perturbation inter-

facial forces can arise only from alterations in the original field distribution arising from transverse motions of the magnetized interface; hence, these waves demonstrate "self-field" effects. In Sec. IV, the complications of nonuniform imposed fields are discussed. These perturbation surface forces can also arise from motions through the initially nonuniform field.

At the outset, the distribution of fields is found, assuming a deflection  $\hat{\xi} = \text{Re } \hat{\xi} \exp(j\omega t - k_y y - k_z z)$ .

#### A. Bulk Fields

Because the equilibrium fields have only x and y components, Eq. (10) becomes ( $D \equiv d(\ )/dx$ ),

$$\zeta_{xx} D^2 \hat{\psi} - j k_y 2 \zeta_{xy} D \hat{\psi} - (k_y^2 \zeta_{yy} + k_z^2 \zeta_{zz}) \hat{\psi} = 0 \quad (22)$$

where it has been assumed that  $\psi = \text{Re } \hat{\psi}(x) \exp j(\omega t - k_y y - k_z z)$ . Substitution shows that Eq. (22) in turn has solutions:

$$\hat{\psi} = e^{qx} ; \quad q = j\gamma \pm \beta \quad (23)$$

where

$$\gamma = k_y \zeta_{xy}^0 / \zeta_{xx}^0$$

$$\beta = \left[ \zeta_{xx}^0 (k_y^2 \zeta_{yy}^0 + k_z^2 \zeta_{zz}^0) - k_y^2 (\zeta_{xy}^0)^2 \right]^{1/2} / \zeta_{xx}^0$$

The pole faces are highly permeable, therefore the perturbation tangential field is taken as zero at their surfaces. This is equivalent to making  $\hat{\psi}(a) = 0$  and  $\hat{\psi}(-b) = 0$ . The appropriate linear combination of solutions from Eq. (23) in each region is then

$$\hat{\psi}_a = A e^{j\gamma_a x} \sinh \beta_a (x-a); \quad \hat{\psi}_b = C e^{j\gamma_b x} \sinh \beta_b (x+b) \quad (24)$$

The constants, A and C, are determined by the interfacial conditions that  $\bar{H}$  tangential and  $\bar{B}$  normal to the interface be continuous. In terms of the normal vector

$\bar{n} \approx \bar{i}_x - (\partial \xi / \partial y) \bar{i}_y - (\partial \xi / \partial z) \bar{i}_z$ , these conditions are

$$\bar{n} \times [\bar{H}^0 - \nabla \psi] = 0 \quad (25)$$

and

$$\bar{n} \cdot [\mu^0 \bar{H}^0 + \mu^1 \bar{H}^0 - \mu^0 \nabla \psi] = 0 \quad (26)$$

respectively at  $x = \xi$ , with  $[F^0] \equiv F^a - F^b$  and  $[\phi] \equiv \phi_a - \phi_b$ . To linear terms, these expressions are satisfied if at  $x = 0$ ,

$$[\psi] = [\bar{H}_x^0] \hat{\xi} \quad (27)$$

and

$$-\mu [\zeta_{xj}^0] \frac{\partial \psi}{\partial x_j} - \frac{\partial \xi}{\partial y} [\mu^0 \bar{H}_y^0] = 0 \quad (28)$$

Direct substitution of Eqs. (24) into these last two expressions gives

$$A = \hat{\xi} \left\{ -\mu_0 [\bar{H}_x^0] \beta_b \zeta_{xx}^b \cosh \beta_b b + j k_y [\mu^0 \bar{H}_y^0] \sinh \beta_b b \right\} / \Delta \quad (29)$$

where

$$\Delta = \mu_0 (\beta_b \zeta_{xx}^b \sinh \beta_a a \cosh \beta_b b + \beta_a \zeta_{xx}^a \cosh \beta_a a \sinh \beta_b b)$$

and a similar expression for C, given by Eq. (29) with all a's and b's interchanged and the sign of the second term reversed. Thus, given the interface geometry, the fields are obtained. The associated interfacial stresses can now be computed.

### B. Magnetization Surface Force Density

The x-directed magnetization surface force density is

$$T_x = [T_{xj}] n_j \approx [T_{xx}] - \frac{\partial \xi}{\partial y} [T_{xy}] \quad (30)$$

which, in view of Eq. (18) requires the linearized forms of  $\mu H_x^2$  and  $w'$  :

$$\mu H_x^2 \approx \mu^0 (H_x^0)^2 - \mu_0 H_x^0 \zeta_{xx}^0 \frac{\partial \psi}{\partial x} - \mu_0 H_x^0 \zeta_{xy}^0 \frac{\partial \psi}{\partial y} - H_x^0 \mu^0 \frac{\partial \psi}{\partial x} \quad (31)$$

$$w' \approx w'[(H^0)^2] - \mu^0 \left( H_x^0 \frac{\partial \psi}{\partial x} + H_y^0 \frac{\partial \psi}{\partial y} \right)$$

Because the equilibrium fields satisfy the condition  $[\mu^0 H_x^0 H_y^0] = H_y^0 [\mu^0 H_x^0] = 0$ , the last term in Eq. (30) vanishes. It follows from the last two equations, after substitution of the traveling-wave form for  $\psi$ , that

$$\hat{T}_x = [-\mu_0 H_x^0 \zeta_{xx}^0 D\psi + jk_y (\mu_0 H_x^0 \zeta_{xy}^0 - \mu^0 H_y^0) \psi] \quad (32)$$

In turn, the surface force density can be related to the surface deflection by using the fields computed in Sec. A., summarized by Eqs. (24) and (29)

$$\begin{aligned} \hat{T}_x = \hat{\xi} \left[ \mu_0^2 [H_x^0]^2 \beta_b \beta_a \zeta_{xx}^b \zeta_{xx}^a \cosh \beta_b b \cosh \beta_a a \right. \\ \left. - k_y^2 [\mu^0 H_y^0]^2 \sinh \beta_b b \sinh \beta_a a \right] / \Delta \quad (33) \end{aligned}$$

where  $\Delta$  is defined with Eq. (29).

Written in the form of Eq. (33), it is evident that the surface force density is either exactly in or out of temporal and spatial phase with the deflection. The effect of the normal field  $H_x^0$  is to increase further a given deflection, while that of  $H_y^0$  is to return the interface to its equilibrium position. This latter force exists only if there are components of the wave propagating in the  $y$  direction. These same qualitative consequences apply to the linear magnetization case with the only difference being that the nonlinearity alters the magnitude of the magnetic field effects on the perturbation interfacial shear.

The dispersion equation follows from the requirement that the surface force-displacement relation of Eq. (33) be consistent with the mechanical equations of motion.

### C. Dispersion Equation

Because there are no magnetic interfacial shear tractions, it serves the present purposes to use an inviscid fluid model. Traveling-wave solutions of the form  $p = \text{Re } \hat{p}(x)e^{j(\omega t - k_y y - k_z z)}$  in the bulk are determined by the conditions that the normal velocity be zero at the pole faces and continuous at the interface, and that the fluid displacement be  $\xi = \text{Re } \hat{\xi} \exp j(\omega t - k_y y - k_z z)$  at the interface. It follows that the complex amplitudes of the perturbation pressures at points  $\alpha$  and  $\beta$  just above and below the interface have the difference:

$$\hat{p}^\alpha - \hat{p}^\beta = -\frac{\omega^2}{k} \hat{\xi} [\rho_a \coth ka + \rho_b \coth kb] + g\hat{\xi}(\rho_b - \rho_a) \quad (34)$$

with  $k = (k_y^2 + k_z^2)^{1/2}$ . The balance of surface forces, as illustrated in Fig. 2, then requires that

$$\hat{p}^\alpha - \hat{p}^\beta = \hat{T}_x - k^2 T \hat{\xi} \quad (35)$$

with  $\hat{T}_x$  the complex amplitude of the magnetic surface force density. The last term arises from the linearization of the surface force density  $T[\partial^2 \xi / \partial y^2 + \partial^2 \xi / \partial z^2]$ , where  $T$  is the surface tension.

Substitution of Eqs. (33) and (34) into Eq. (35), with the requirement that  $\hat{\xi} \neq 0$ , gives the desired dispersion equation for waves on the interface.



$$\omega^2 \rho_{eq} = gk(\rho_b - \rho_a) + k^3 T - \frac{k}{\Delta} \left[ \mu_o^2 \|H_x^o\|^2 \beta_b \beta_a \zeta_{xx}^b \zeta_{xx}^a \cosh \beta_b b \cosh \beta_a a \right. \\ \left. - k_y^2 \|\mu_o H_y^o\|^2 \sinh \beta_b b \sinh \beta_a a \right] \quad (36)$$

where  $\rho_{eq} = \rho_a \coth ka + \rho_b \coth kb$

$$\Delta = \mu_o \left[ \beta_b \zeta_{xx}^b \sinh \beta_a a \cosh \beta_b b + \beta_a \zeta_{xx}^a \cosh \beta_a a \sinh \beta_b b \right]$$

Attention is now given to motions resulting from particular orientations of the imposed fields. The general relation, Eq. (36), shows that although magnetization of the fluid in one direction can produce a saturation coupling to fields in another direction, the interfacial dynamics resulting from an imposed field of arbitrary orientation are essentially a superposition of effects due to the tangential and perpendicular field components. This is not quite true, of course, because the parameters  $\beta$  and  $\zeta_{ij}$  depend on both field components. For qualitative purposes and for presently available fluids, however, this gives a fair picture of the dynamics.

#### D. Perpendicular Field Waves and Instabilities

In the case of a magnetic liquid bounded from above by a nonmagnetic gas or liquid, and stressed by a perpendicular field, parameters in Eq. (36) reduce to

$$H_y^o = 0 ; \quad \zeta_{xx}^a = \zeta_{yy}^a = \zeta_{zz}^a = 1 ; \quad \zeta_{yy}^b = \zeta_{zz}^b = \chi + 1 \\ \mu^a = \mu_o ; \quad \zeta_{xy}^a = \zeta_{xy}^b = 0 ; \quad \beta_a = k \\ \beta_b = k\eta ; \quad \zeta_{xx}^b = \chi_s + 1 \quad (37)$$

where it is convenient to define

$$\eta = [(1 + \chi)/(1 + \chi_s)]^{1/2} ; \quad M_x^b = \chi H_x^b \quad (38)$$

In this case, Eq. (36) reduces to

$$\omega^2 \rho_{eq} = gk(\rho_b - \rho_a) + k^3 T - \mu_o (M_x^b)^2 k^2 / \left\{ \tanh ka + [\tanh (k\eta b)] / \eta (\chi_s + 1) \right\} \quad (39)$$

As for the case of a linear magnetization characteristic, the phase velocity of interfacial waves is reduced by the magnetic field. In the limit in which the pole faces are well removed from the interface ( $k\eta b \gg 1$ ,  $ka \gg 1$ ), Eq. (39) shows that there is a static instability that first occurs at the Taylor wavelength  $2\pi/k^*$ ,  $k^* = \sqrt{g(\rho_b - \rho_a)/T}$  as  $M_x^b$  is raised to the critical value:

$$(M_x^b)^* = \left\{ \frac{2k^* T}{\mu_o} [1 + 1/\eta (\chi_s + 1)] \right\}^{1/2} \quad (40)$$

These last deductions are those calculated and experimentally verified by Cowley and Rosensweig (1967). Note that Eq. (39) implies that there is an exchange of stabilities, i.e., that the instability is incipient with  $\omega = 0$ .

In Sec. VI, further support will be given to the model through an experiment in which the wavelength (and hence  $k$ ) is essentially fixed, and the dependence of the frequency on  $M_x^b$ , as given by Eq. (39), verified.

#### E. Tangential Field Surface Waves

With  $H_x^o = 0$  and the equilibrium  $\bar{H}$  tangential to the interface, there is a tendency for waves propagating along the field lines to be stiffened; to propagate more rapidly. Parameters in region (a) are as for Sec. D, and in region (b)

$$\begin{aligned} \zeta_{xx}^b &= \zeta_{zz}^b = \chi + 1 ; \quad \zeta_{xy}^b = 0 ; \quad M_y^b = \chi H_y^b \\ \zeta_{yy}^b &= \chi_s + 1 ; \quad \beta_b = \left[ \left( \frac{\chi_s + 1}{\chi + 1} \right) k_y^2 + k_z^2 \right]^{1/2} \end{aligned} \quad (41)$$

Thus, the dispersion equation becomes:

$$\omega^2 \rho_{eq} = gk(\rho_b - \rho_a) + k^3 T + \frac{\mu_0 k^2 (M_y^b)^2}{[(\chi + 1)\beta_b (\coth \beta_b b)/k + \coth ka]} \quad (42)$$

As for the magnetically linear case, self-field effects are absent for perturbations propagating across the lines of field intensity. In Sec. VI, an experiment will show the upward shift in frequency of a given wavelength predicted by Eq. (42) as a function of  $M_y^b$ .

#### IV Systems of Homogeneous Liquids: Nonuniform Fields

The ferrohydrodynamics of interfaces in uniform imposed fields, as developed in Sec. V, involves the self-consistent interaction of fields and fluids. The perturbation in the magnetic surface force density in this case arises from alterations of the field distribution caused solely by distortions of the fluid interface. On the other hand, if a nonuniform field is present, the force perturbations can also arise simply from displacements of the interface through the imposed field. (See Calvert and Melcher, 1969, for a discussion of "self-field" and "imposed-field" effects.)

Gradients in the imposed field are a consequence of field "curvature". Examples are shown in Fig. 3, where the perpendicular and tangential field configurations are illustrated in cylindrical geometry for an interface having the equilibrium radius of curvature,  $R$ .

It is not the objective here to develop the details of any given non-uniform field configuration, but rather to highlight the essential features of the dynamics in nonuniform fields by representing the field gradient effects in terms of quasi-one-dimensional models. In the following, it is still assumed that the interface is initially flat (Fig. 2) but that the imposed field components vary spatially with the  $x$  direction. Of course, cartesian field components that vary with only one spatial coordinate cannot be both solenoidal and irrotational. However, by judicious approximations, aimed at representing

situations such as those shown in Fig. 3 where the field does have curvature but where interfacial wavelengths are small compared to the radius of curvature, physically meaningful results can be obtained without becoming involved in the details of Bessel's functions, spherical harmonics, etc. The quasi-one-dimensional <sup>model</sup> summarizes the salient features of a wide class of configurations, because the detailed nature of the field nonuniformity is de-emphasized. The local effects of nonuniformities found in cylindrical, spherical or other geometries are equally well represented by simply evaluating the appropriate local gradients.

Because the fields are nonuniform, the susceptibility  $\chi$  is a function of position in the bulk of the liquids. Even so, with the force density representation of Eq. (17), the coupling between fluid and field remains confined to the interface.

#### A. Boussinesq Approximation

In the fluid bulk,  $\alpha'_i = 0$  and the magnetic field distribution is again predicted by Eq. (10), which becomes

$$\frac{\partial \zeta_{jk}^0}{\partial x_j} \frac{\partial \psi}{\partial x_k} + \zeta_{jk}^0 \frac{\partial^2 \psi}{\partial x_j \partial x_k} = 0 \quad (43)$$

Because the imposed fields are a function of  $x$  alone,  $\zeta_{jk}^0 \equiv \zeta_{jk}^0(x)$ .

Thus, Eq. (43), although linear, has coefficients that depend on  $x$ .

In the following, the coefficients in Eq. (43) are approximated by constants evaluated at the equilibrium position of the interface, e.g.,  $\zeta_{jk}^0(x) \rightarrow \zeta_{jk}^0(0) = \zeta_{jk}^c$ . With this approximation, familiar from the literature for thermal convection instability (Boussinesq, 1903), Eq. (43) becomes the constant coefficient expression

$$(D\zeta_{xk})^c \frac{\partial \psi}{\partial x_k} + \zeta_{jk}^c \frac{\partial^2 \psi}{\partial x_j \partial x_k} = 0 \quad (44)$$

The "Boussinesq" approximation is particularly well justified here because coefficients are evaluated at the interface, and the surface wave solutions of interest tend to be confined to the neighborhood of the interface. Note that the first term in Eq. (44) vanishes unless the fluid is both magnetically nonlinear and stressed by a nonuniform field.

### B. Perpendicular-Field Gradient Effects

If the imposed field takes the form  $\vec{H}^0 = H_x^0(x) \vec{i}_x$ , Eq. (44) reduces to

$$D^2 \hat{\psi} + \left[ (D\zeta_{xx})^c / \zeta_{xx}^c \right] D \hat{\psi} - (\mu^c k^2 / \mu_0 \zeta_{xx}^c) \hat{\psi} = 0 \quad (45)$$

where it has been assumed that  $\psi = \text{Re } \hat{\psi}(x) \exp j(\omega t - k_y y - k_z z)$ . It follows that solutions in the respective regions are

$$\hat{\psi}_{(\frac{a}{b})} = A_{(\frac{a}{b})} e^{-\sigma x} \sinh \delta \left[ x + \left( \frac{-a}{b} \right) \right] \quad (46)$$

with  $\sigma$  and  $\delta$  defined in the appropriate regions as

$$\sigma = (D\zeta_{xx})^c / 2\zeta_{xx}^c ; \quad \delta = \left[ \sigma^2 + (\mu^c k^2 / \mu_0 \zeta_{xx}^c) \right]^{1/2} \quad (47)$$

Note that the solutions, Eqs. (46), have been chosen to satisfy the boundary conditions at  $x = a$  and  $x = -b$ , discussed in Sec. IIIA. Even though the equilibrium field is now spatially varying, the linearized conditions at  $x = 0$  reduce to Eqs. (27) and (28), with the latter reducing further to  $\llbracket \zeta_{xx}^c D \hat{\psi} \rrbracket = 0$ . Substitution gives the constants  $A_a$  and  $A_b$  in terms of  $\xi$  in a form similar to Eq. (29).

The magnetization force density is found by following steps familiar to those of Eqs. (30)-(33). Now the equilibrium part of  $T_{xx}$  is a function of  $x$  and, as it is evaluated at the perturbed position of the interface, contributes a perturbation term proportional to  $\hat{\xi}$ . Thus, Eq.(30) becomes

$$\hat{T}_x = \hat{\xi} [D(\mu^o H_x^o)]^c [H_x^c] - [\mu_o \zeta_{xx}^c H_x^c D\psi] \quad (48)$$

Because  $\hat{\psi}$  has been evaluated in terms of  $\hat{\xi}$ , this expression, together with Eq. (34), can be introduced into the stress balance equation (35), to give an expression that is homogeneous in  $\hat{\xi}$ . The dispersion equation follows from the condition that the coefficient of  $\hat{\xi}$  vanish.

$$\begin{aligned} \omega^2 \rho_{eq} = & gk(\rho_b - \rho_a) + k^3 T - k [D(\mu^o H_x^o)]^c [H_x^c] \\ & - k \mu_o \zeta_{xx}^a \zeta_{xx}^b [H_x^c]^2 / [\zeta_{xx}^b (\sigma_a + \delta_a \coth \delta_a)^{-1} + \zeta_{xx}^a (-\sigma_b + \delta_b \coth \delta_b)^{-1}] \end{aligned} \quad (49)$$

In this expression,  $\zeta_{xx}^c$  evaluated in regions (a) and (b) is written as  $\zeta_{xx}^a$  and  $\zeta_{xx}^b$ .

In interpreting this expression, remember that each term arises because of a perturbation surface force density. The last term is attributable to the mutual coupling between field and fluid and is negative. Although the field nonuniformity does play a quantitative role, the self-field effects are qualitatively the same destabilizing influence as for a uniform imposed field.

The third term in Eq. (49) reflects the "imposed" field effect. It is present because of the change in magnetic stress experienced by the interface as it is displaced into a region of greater or lesser field intensity. For example, if fluid (a) of Fig. 3a is magnetic, while that of (b) is not, then there is a magnetic surface force acting downward on the interface in proportion to  $(H_x^o)^2$  at the interface. Suppose that  $[D\mu^o H_x^o]^c > 0$ , as in the case

illustrated. Then an upward excursion of the interface is accompanied by an increase in the local downward directed magnetic stress, hence a magnetic surface force that tends to restore the equilibrium. This stabilizing effect is consistent with Eq. (49), because in the example  $[\![H_x^c]\!] < 0$ , which implies that the third term tends to make  $\omega^2$  positive. Specifically, for the example in cylindrical coordinates,  $\mu^0 H^0 = B_0 R / (R - x)$ , ( $B_0$  the equilibrium radial flux density at the interface) requires the third term in Eq. (49) to become:

$$-k[D(\mu H_x)]^c [\![H_x^c]\!] = -\frac{k B_0^2}{R} [\![\frac{1}{\mu^c}]\!] \quad (50)$$

If fluid (a) is magnetic while (b) is not,  $[\![1/\mu^c]\!]$  is negative and the term on the right in Eq. (50) is positive; hence it stabilizes the interface.

### C. Tangential Field-Gradient Stabilization

Field configurations characterized by Fig. 3b are modeled by the planar interface of Fig. 3d, with the imposed field a function of  $x$ . The dispersion equation follows from steps similar to those of the previous section. Instead of Eq. (45), Eq. (44) reduces to

$$D^2 \hat{\psi} + \frac{(D\mu^0)^c}{\mu^c} D\hat{\psi} - [(k_y^2 \zeta_{yy}^c \mu_0 / \mu^c) + k_z^2] \hat{\psi} = 0 \quad (51)$$

so that, although solutions take the same form as in Eqs. (46), the parameters governing the spatial distribution of  $\hat{\psi}$  are

$$\sigma = (D\mu^0)^c / 2\mu^c ; \quad \delta = \left[ \sigma^2 + (k_y^2 \zeta_{yy}^c \mu_0 / \mu^c + k_z^2) \right]^{1/2} \quad (52)$$

Linearized boundary conditions for the fields are again as given by Eqs. (27) and (28), which reduce to

$$[\![\hat{\psi}]\!] = 0 \quad ; \quad [\![\mu^c D\hat{\psi}]\!] = j k_y \xi_{H_y}^c [\![\mu^c]\!] \quad (53)$$



These serve to fix the coefficients  $A_a$  and  $A_b$ , and hence  $\hat{\psi}$ .

The perturbation magnetic force density, linearized to include the non-uniform imposed field, has the complex amplitude

$$\hat{T}_x = -\frac{1}{2} \hat{\xi} [\mu^c [D(H_y^0)^2]^c] - j k_y [\hat{\psi} \mu^c H_y^c] \quad (54)$$

Finally, the dispersion equation follows as in previous sections by substituting Eq. (54), with  $\hat{\psi}$  written in terms of  $\hat{\xi}$ , together with Eq. (34), into Eq. (35)

$$\begin{aligned} \frac{\omega^2}{k} \rho_{eq} = & g(\rho_b - \rho_a) + k^2 T + \frac{1}{2} [\mu^c [D(H_y^0)^2]^c] \\ & + k_y^2 (H_y^0)^2 [\mu^c]^2 / [\mu_a^c (\sigma_a + \delta_a \coth \delta_a a) + \mu_b^c (-\sigma_b + \delta_b \coth \delta_b b)] \end{aligned} \quad (55)$$

The last term in Eq. (55) shows that the self-field effects, although somewhat modified by the saturation effects of the nonuniform field distribution, always tend to stabilize perturbations that propagate along the lines of magnetic field intensity. The third term on the right has a physical origin similar to that of the imposed field term discussed in the previous section; it can tend to stabilize or destabilize the interface, according to the sign of the gradient in field intensity.

In the cylindrical example of Fig. 3b, field gradients are such that if fluid (a) is magnetic and (b) is not, the field tends to produce a stable equilibrium. In particular, the equivalent cartesian field is  $H_y^0 = H_0 R / (R - x)$ , and the third term of Eq. (55) becomes:

$$\frac{1}{2} [\mu^c [D(H_y^0)^2]^c] = H_0^2 [\mu] / R \quad (56)$$

The most critical interfacial disturbances are those propagating across the lines of equilibrium field intensity ( $k_y = 0$ ) and a condition that all wavelengths be stable follows from Eq. (55) as

$$\frac{1}{2} \mu^c [D(H_y^0)^2]^c > g(\rho_a - \rho_b) \quad (57)$$

Thus, the field gradient can be used to stabilize the equilibrium even with the heavier fluid "on top". This type of field-gradient stabilization has assumed importance in dielectrophoretic orientation systems (Melcher & Hurwitz, 1967).

#### D. Concentrated Field-Gradient Stabilization

In Sec. IVC, it is assumed that the field gradient is small and comparable in effect to the "self-fields" in its influence. By contrast, consider the situation shown in Fig. 4a, where magnetic sheets having the spacing  $s$  are used in conjunction with a magnetic circuit to produce an imposed field with a gradient that is large in the neighborhood of the equilibrium interface, but essentially zero at adjacent points removed a distance  $s$  or more from the interface. (For simplicity, it is assumed that the interface does not reach the neighborhood of the upper fringing field.) If the spacing,  $s$ , between sections of the magnetic circuit is made small, this configuration can give imposed-field effects much larger than those due to the self fields. Hence, the latter are ignored in the following remarks.

As the interface passes through the fringing field region, the magnetic surface force experienced by the interface switches from fully "on" to fully "off" within a displacement on the order of the spacing,  $s$ . Thus, the configuration is sometimes referred to as being of the "bang-bang" type.

Analogous dielectrophoretic interactions with concentrated field gradients have been discussed elsewhere (Melcher, Hurwitz & Guttman, 1968). Attention is confined here to indicating the simple generalizations of the electrohydrodynamic models required to account for nonlinear magnetization characteristics.

Interfacial oscillations and instabilities in cases like that of Fig. 4a can be represented with a surprising degree of accuracy by the equivalent pendulum of Fig. 4b. The lengths,  $l_a$  and  $l_b$ , of the fluid columns are selected to approximate the inertial and gravitational characteristics of the mode to be represented. It is assumed that the magnetic segments do not impede the flow mechanically; an assumption that is most appropriate to motions in the  $x-z$  plane.

Pendulum motions are coupled to the magnetic field only at the interfaces. Thus, Bernoulli's equation shows that,

$$(\rho_a l_a + \rho_b l_b) \frac{d^2 \xi}{dt^2} = 2(\rho_a - \rho_b) g \xi + \tau_x(\xi) \quad (58)$$

where  $\tau_x$  is the total magnetic force (per unit  $y$ - $z$  area) acting at the interfaces. Analog measurements (Guttman, 1967) show that a useful model represents the variation of the imposed  $H_y^2$  as a linear transition from  $(H^m)^2$  starting as  $x = s/2$  and ending as  $H_y = 0$  at  $x = -s/2$ , as shown in Fig. 5a. The field is essentially the constant  $H^m$  between the segments. In accordance with the assumption that the effect of the fluid on the field is negligible, this distribution remains unaltered in the face of the fluid motions.

The surface force density  $T_x$  acting on the right interface of the pendulum (Fig. 4b) is  $T_x = [T_{xx}]$  with  $T_{xx}$  from Eq. (18) given as  $T_{xx} = -w'$ . That is,

$$T_x = -\frac{1}{2} \int_0^{H^2(\xi)} [\mu] \delta H^2 \quad (59)$$

with  $H^2$  given by Fig. 5a, evaluated at the interface; where  $x = \xi$ . Note that  $T^m$  is simply Eq. (59) with the upper limit of integration  $(H^m)^2$ .

As illustrated by the typical characteristics of Fig. 1, the effect of increasing  $H^2$  is to decrease  $\mu$ . Thus, the saturation magnitude of the surface force,  $T^m$ , is less than is obtained if  $\mu$  were constant at its zero field value.

The typical variation of  $T_x$  is sketched in Fig. 5b.

The total magnetic force per unit area on the pendulum  $\tau_x$  is the sum of the surface force densities from the two interfaces, as sketched in Fig 5c. Like the dispersion equations of the previous sections, the equivalent pendulum can be used to predict frequencies of oscillation and conditions for instability. Further, the neglect of self-fields makes it possible to account for large amplitude effects. Given the fluid characteristics, and  $H^m$  and  $s$ , the dependence of  $\tau_x$  on  $\xi$  is known, and the pendulum motions are simply represented in terms of a potential well. This approach to investigating the large-amplitude oscillations has been presented in the discussion of dielectrophoretic concentrated field interactions (Melcher, Guttman & Hurwitz, 1968). Note that the saturation magnetic stress,  $T^m$ , assumes the role played by  $\frac{1}{2}\mu(H^m)^2$  in the linear case. For many engineering purposes, it is appropriate to represent the large amplitude effects by approximating the transition region of Fig. 5c by a straight line, saturating at  $\tau_x = \pm T^m$ . This model would be useful in dealing with the magnetic analog to dielectrophoretic "wall-less pipes" (Melcher, Hurwitz, and Fax, 1969).

The stability of the equivalent pendulum against small amplitude oscillations is investigated by linearizing  $\tau_x$  at  $\xi = 0$ ; from Eq. (59),

$$\tau_x = 2 \frac{\partial T_x}{\partial \xi} (\xi = 0) = - \xi \left[ \mu \right] \left| \frac{(H^m)^2}{s} \right|_{H^2 = (H^m/2)^2} \quad (60)$$

Substitution of this expression into Eq. (58) shows that the equilibrium is stable if

$$\frac{1}{2} \left[ \mu \right] \frac{(H^m)^2}{s} > (\rho_a - \rho_b)g \quad (61)$$

Note that, with the understanding that  $\mu$  is evaluated at  $H = H^m/\sqrt{2}$ , this is

just the condition given by Eq. (57). Those perturbations that are most critical for interfacial stability in Sec. IVC ( $k_y = 0$ ) do not lead to self-fields, so the equivalence of Eqs. (57) and (61) is not surprising.

## VI. Experiments

Three experiments serve to support the analytical models developed in the previous section. They are similar to studies that have been reported in dielectrophoretic fluid dynamics (Devitt & Melcher, 1965), (Melcher & Hurwitz, 1967).

### A. Perpendicular Field Surface Waves

Convenient experiments for verifying the dispersion relations for tangential and normally applied magnetic fields use boundary conditions to impose a particular wavelength on the ferrofluid interface, and consist of the measurement of the shift in resonance frequency resulting from additions of magnetic field. A schematic representation of the experiment for the perpendicular field case is shown in Fig. 6, together with the frequency shift data that is the object of the experiment.

Rectangular containers, partially filled with ferrofluid, are driven by a low frequency transducer to vibrate in the horizontal plane. By shaking the container at appropriate frequencies, it is possible to elicit resonances near the natural frequencies of the interface. These occur as the box contains an integral number,  $n$ , of half-wavelengths over its length such that  $k_y = n\pi/l$ , with the one-dimensional drive effective in constraining  $k_z$  to be essentially zero. Container dimensions in the horizontal plane are given in the figure legend with the data.

The magnetic field is produced by Helmholtz coils, driven by an adjustable source of current in series with an ammeter which is calibrated to give the required field intensity at the interface. The experimental procedure is identical for this and for the experiment of the next section. In all cases, the fluid

depth is great enough to make effects of the container bottom negligible.

In a typical measurement, the resonance condition is established by varying the driving frequency so as to approach the resonance once from above and once from below. The resulting data are shown in Fig. 6.

In this normal field experiment, there is an inadvertent gradient in the imposed magnetic field intensity at the interface; therefore, the prediction provided by Eq. (49) is appropriate, in the limit where  $\mu^a \rightarrow \mu_0$ ,  $\sigma_a \rightarrow 0$ ,  $\delta_a \rightarrow k$ ,  $a \rightarrow \infty$ , and  $b \rightarrow \infty$ . If the frequency in the absence of the magnetic field is defined as  $\omega_0$ , then Eq. (49) predicts that

$$\left| \frac{\omega_0^2 - \omega^2}{\omega_0^2} \right|^{1/2} = \left| \frac{k\chi^c [D(\mu H_x)^2]^c}{2\mu_0(\chi^c + 1)\omega_0^2 \rho} - \frac{\mu_0 (M_x^c)^2 k^2}{\omega_0^2 \rho [1 + k/(\chi_s^c + 1)(\delta_b - \sigma_b)]} \right|^{1/2} = F_p \quad (62)$$

This expression is the basis for the solid curve shown in Fig. 6. The discrepancy between theory and experiment is of an order expected from sources of experimental error. Typically, the resonance frequency is measured with confidence limits of  $\pm 5\%$ . Calibration errors are particularly troublesome because ohmic heating of the field coils introduces errors as great as 10% in the inference of field intensities from coil current. Finally, the flat equilibrium geometry of the interface is difficult to maintain at higher fields; a direct reflection of field-gradient effects not accounted for and a source of error in establishing the proper value of  $k$ . Sufficiently short wavelength modes are represented in the data of Fig. 6 that the self-field effects dominate the gradient effects; the gradient term in Eq. (62) represents a correction under the experimental conditions.

Ultimately, the downward shift in resonance frequency is terminated by interfacial instability as the frequency reaches zero, and Eq. (40) is satisfied. With increasing magnetization, the instability condition is first met

for a mode having the Taylor wavelength. This self-field instability is the subject of the careful investigations of Cowley and Rosensweig and appears to have a threshold which is well understood.

### B. Tangential Field Surface Waves

With the tangential field experiment shown in Fig. 7, the resonance frequencies shift upward with increasing magnetization. The data shown result from experimental procedures similar to those discussed in Sec. A. In this experiment, nonuniformities in the imposed field are not significant, and Eq. (42) suffices to predict the frequency shifts. Again, theory and experiment are within an agreement consistent with sources of experimental error.

### C. Tangential-Field Gradient Stabilization

A dramatic demonstration of ferrofluid dynamics consists of simply suspending the liquid in the top of a partially filled plastic container with the field from a small permanent magnet. This is the classic configuration of a liquid suspended over a gas. The magnetic field easily prevents Rayleigh-Taylor instability.

It should be clear from the discussion of uniform field interactions that the self-field effect cannot account for stabilization of the "upside-down" interface. In a perpendicular field, instability rather than stability is a consequence of the uniform field. In a tangential field, interfacial perturbations propagating across the field lines are not stabilized by the field. However, gradients in the imposed field make it possible to retain a stable equilibrium of the liquid over the gas, even with modest fields and gradients. Note that the magnetic field is not used to support the fluid, rather just to stabilize the fluid interface.



The experiment shown in Fig. 8 demonstrates this gradient stabilization. Note that the apparatus assumes essentially the geometry of Fig. 3b, with Eqs. (56) and (57) giving a theoretical prediction of the condition for instability. Each experimental point represents a different equilibrium position of the surface, such that  $H_0$  of Eq. (56) is proportional to  $1/R$  and to the current,  $i$ , in the field coils. This is the basis for the solid curve in Fig. 8.

To obtain the data points shown, the field magnitude and gradient are established by calibration curves at five positions over the 1 - 5 cm. vertical extent of the fluid volume. The fluid is injected between the magnetizable plates until the set amount of current is no longer able to stabilize the equilibrium. It is important that at all times the upper section of the container is maintained leak-tight, so that the field is not used to support the liquid. At the point of instability, the liquid suddenly runs down the four edges of the container. The value of  $R$  (see Fig. 3b) at which this occurs, along with the current setting, then constitutes a data point on Fig. 8, indicated by a circle. Alternatively, some data points (squares) are obtained by holding the fluid volume fixed, and reducing the current until instability is observed.

Experimental results and theoretical predictions are well within the bounds expected from sources of experimental error.

## VII. Concluding Remarks

Many interactions between a ferrofluid and a magnetic field involve a single homogeneous liquid with one or more free surfaces. The developments given here emphasize that, even including effects of nonuniform fields and magnetic saturation, these are surface interactions. Although major theoretical attention is given here to including effects of nonlinear magnetization characteristics,

in retrospect it can be recognized that, for many purposes, including an approximate prediction of the experimental results reported in Sec. VI, a judicious choice of magnetization parameters makes it possible to predict the essential features of the dynamics from a theory based on an equivalent linear magnetization characteristic. For example, Eqs. (39) and (42) are in many cases not altered greatly if  $\beta_b \rightarrow k$ ,  $\chi_s \rightarrow \chi$  and  $\eta \rightarrow 1$ , provided that the actual (saturated) susceptibility,  $\chi$ , is used to evaluate the magnetization. The equivalent linear theory must incorporate the actual magnetization or it is likely to be grossly in error.

Although the situations investigated in Sec. III and beyond represent surface interactions, the formulation given in Sec. II provides a convenient starting point for the investigation of bulk instability and internal ferrohydrodynamic waves as found in inhomogeneous fluids. An important class of interactions in this category involves fluids subject to combined thermal and magnetic stress - especially if the temperature extremes in the fluid bulk bracket the Curie point. Again, there is precedent for such studies from work in electrohydrodynamics (Turnbull & Melcher, 1969).

---

#### Acknowledgments:

Experimental work on the ferrofluids would not have been possible without the cooperation of Dr. R. E. Rosensweig, who made available the laboratory facilities of Avco Corporation, Space Systems Division. Dr. R. Kaiser and Mr. N. Sheppard were of assistance in performing the experiments. Portions of this work were supported by NASA Grant NGL-22-009-014.

## References

- Boussinesq, J., 1903, Theorie Analytique de la Chaleur, Gauthier-Villars, Paris, Vol. 2, p. 172.
- Calvert, R. T., and Melcher, J. R., "Stability and Dynamics of Rotating Dielectrophoretic Equilibria", in publication, J. Fl. Mechanics.
- Cowley, M. D., and Rosensweig, R. E., 1967 J. Fluid Mech., 30, 671.
- Devitt, E. B., and Melcher, J. R., 1965 Phys. Fluids, 8, 1193.
- Guttman, D. S., "Bang-Bang Electrohydrodynamic Stabilization", M.I.T. Department of Electrical Engineering M.S. Thesis, 1967.
- Melcher, J. R., 1963, Field-Coupled Surface Waves, M.I.T. Press, Cambridge, Massachusetts
- Melcher, J. R., and Hurwitz, M., 1967 J. Spacecraft and Rockets, 4, 864.
- Melcher, J. R., Guttman, D. S., and Hurwitz, M., 1968, J. Spacecraft and Rockets, in publication.
- Melcher, J. R., Hurwitz, M., & Fax, R. G., 1969, J. Spacecraft and Rockets, in publication.
- Neuringer, J. L., and Rosensweig, R. E., 1964, Phys. Fluids 7, 1927.
- Penfield, P. E., Jr., & Haus, H. A., 1967, Electrodynamics of Moving Media, M.I.T. Press, Cambridge, Mass.
- Pohl, H. A., 1960, Sci. Ameri. 203, 107.
- Resler, E. L., Jr. & Rosensweig, R. E., 1967 J. Eng. for Power, Trans. of ASME, July, 399.
- Rosensweig, R. E., 1966<sup>a</sup>, International Sci. Tech. 55, 48.
- Rosensweig, R. E., 1966<sup>b</sup>, AIAA Journal, 4, 1751.
- Rosensweig, R. E., Miskolczy, G., & Ezekiel, F. D., 1968, Machine Design, March, 145.
- Stratton, J.A., 1941, Electromagnetic Theory, McGraw-Hill Book Co., Inc., 145.

References (continued)

Turnbull, R. J., & Melcher, J. R., 1969, Phys. Fluids, in publication

Woodson, H. H., & Melcher, J. R., 1968<sup>a</sup>, Electromechanical Dynamics: Part I, Discrete Systems, John Wiley & Sons, Inc., N. Y., Chap. 3

Woodson, H. H., & Melcher, J. R., 1968<sup>b</sup>, Electromechanical Dynamics: Part II, Fields, Forces and Motion, John Wiley & Sons, Inc., N. Y., 450-463.

### List of Figure Captions

- Fig. 1 Fluid magnetization density,  $M$ , as a function of the imposed magnetic field intensity  $H$ . The inserts show the dependence of  $\chi$  and  $\chi_s$  on  $H$ .
- Fig. 2 Cross-sectional view of initially planar interface between magnetized liquids (a) and (b). Current sheets at  $x = -b, a$ , as well as excitation currents for the magnetic circuit, induce the initially uniform fields  $\vec{H}^a$  and  $\vec{H}^b$ .
- Fig. 3 Examples of nonuniform equilibrium fields: a) Field perpendicular to interface; b) Field tangential to interface; c) Quasi-one-dimensional model for (a); (d) Model for (b).
- Fig. 4 a) Interface between fluids (a) and (b) interacts with field gradient concentrated in neighborhood of equilibrium interface.  
b) Pendulum model for (a).
- Fig. 5 a) Variation of imposed field intensity according to the quasi-one-dimensional model for concentrated field gradient configuration of Fig. 4.  
b) Magnetic surface force density on right interface in Fig. 4(b).  
c) Total magnetic force (per unit  $y$ - $z$  area) on equivalent pendulum of Fig. 4(b).
- Fig. 6 a) Apparatus for measuring resonance frequencies with field imposed perpendicular to interface; vibrations of the tank in the horizontal plane drive the waves.  
b) Relative frequency shift as a function of the parameter  $F_p$ , proportional to the applied field intensity. The frequency shifts downward as the applied field intensity is increased.

Fig. 7 a) Apparatus for measuring resonance frequencies in tangential field  
 b) Relative frequency shift as a function of  $F_t$ , a parameter proportional to the imposed magnetic field intensity.  $F_t$  is defined as the square root of the last term in Eq. (42) divided by  $\omega_0/\rho$ .

Fig. 8 a) Apparatus for measuring conditions for instability on interface in adverse gravitational acceleration. Magnetized steel plates provide the gradient in imposed field intensity required to stabilize the interface.  
 b) Conditions under which incipient instability is observed.  $R$  is the distance from the interface to the point at which the inner surfaces of the steel plates would converge if extended upward, while  $i$  is the magnet current. The solid curve is predicted by Eq. (57).

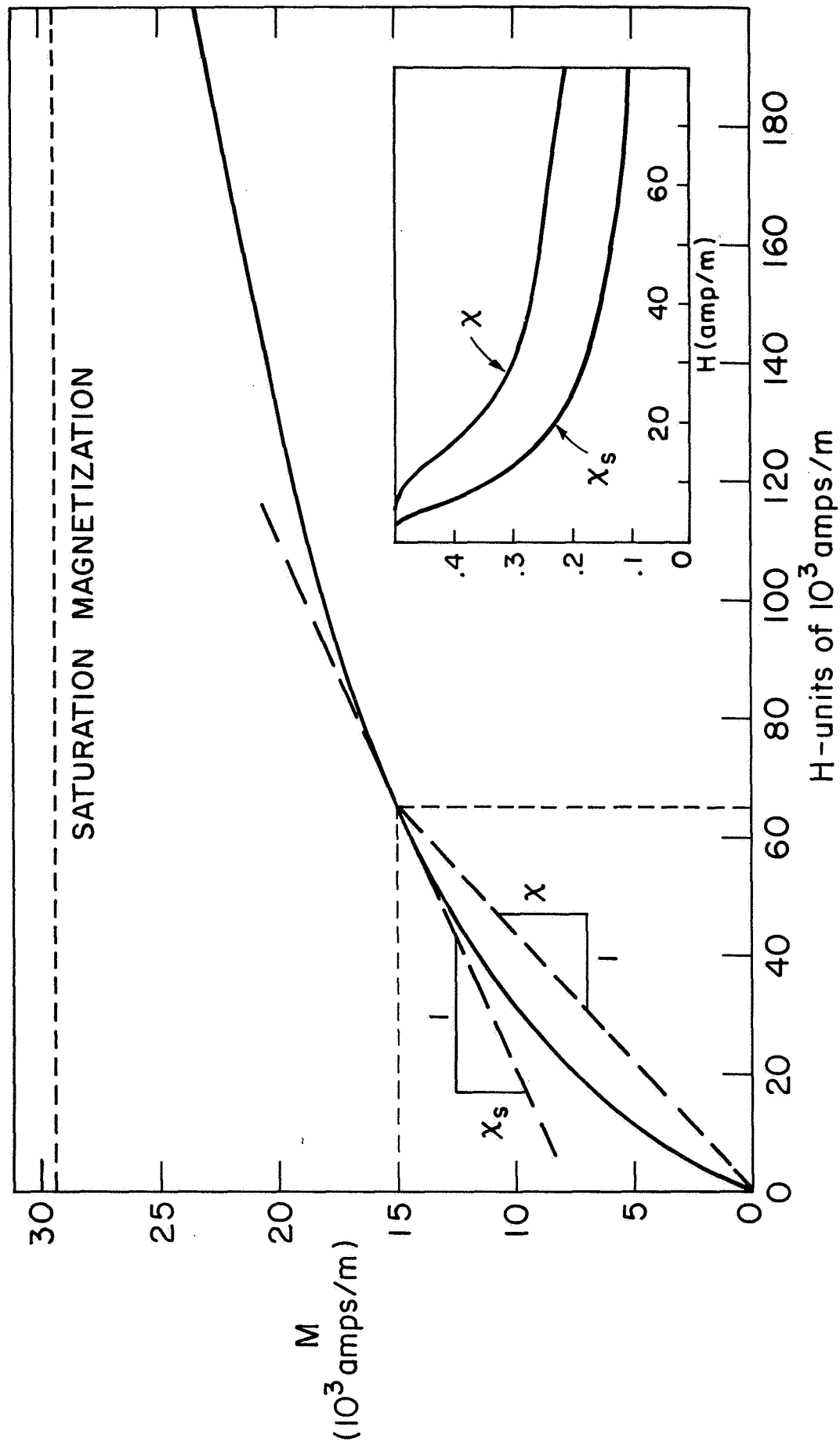


**Fig. 1** Fluid magnetization density,  $M$ , as a function of the imposed magnetic field intensity  $H$ . The inserts show the dependence of  $\chi$  and  $\chi_s$  on  $H$ .



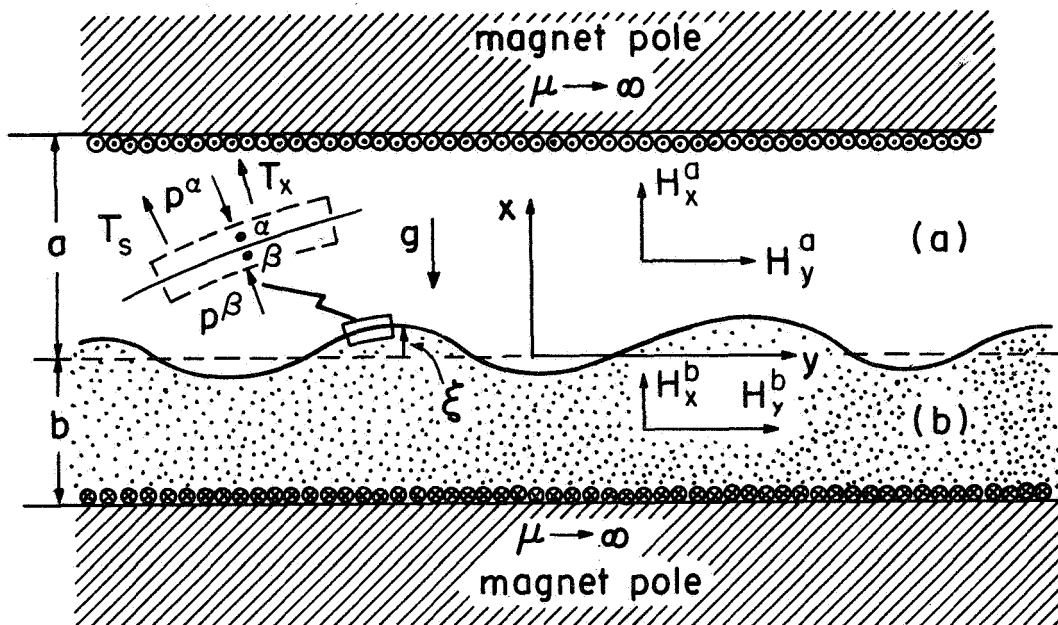


Fig. 2 Cross-sectional view of initially planar interface between magnetized liquids (a) and (b). Current sheets at  $x = -b, a$ , as well as excitation currents for the magnetic circuit, induce the initially uniform fields  $\vec{H}^a$  and  $\vec{H}^b$ .

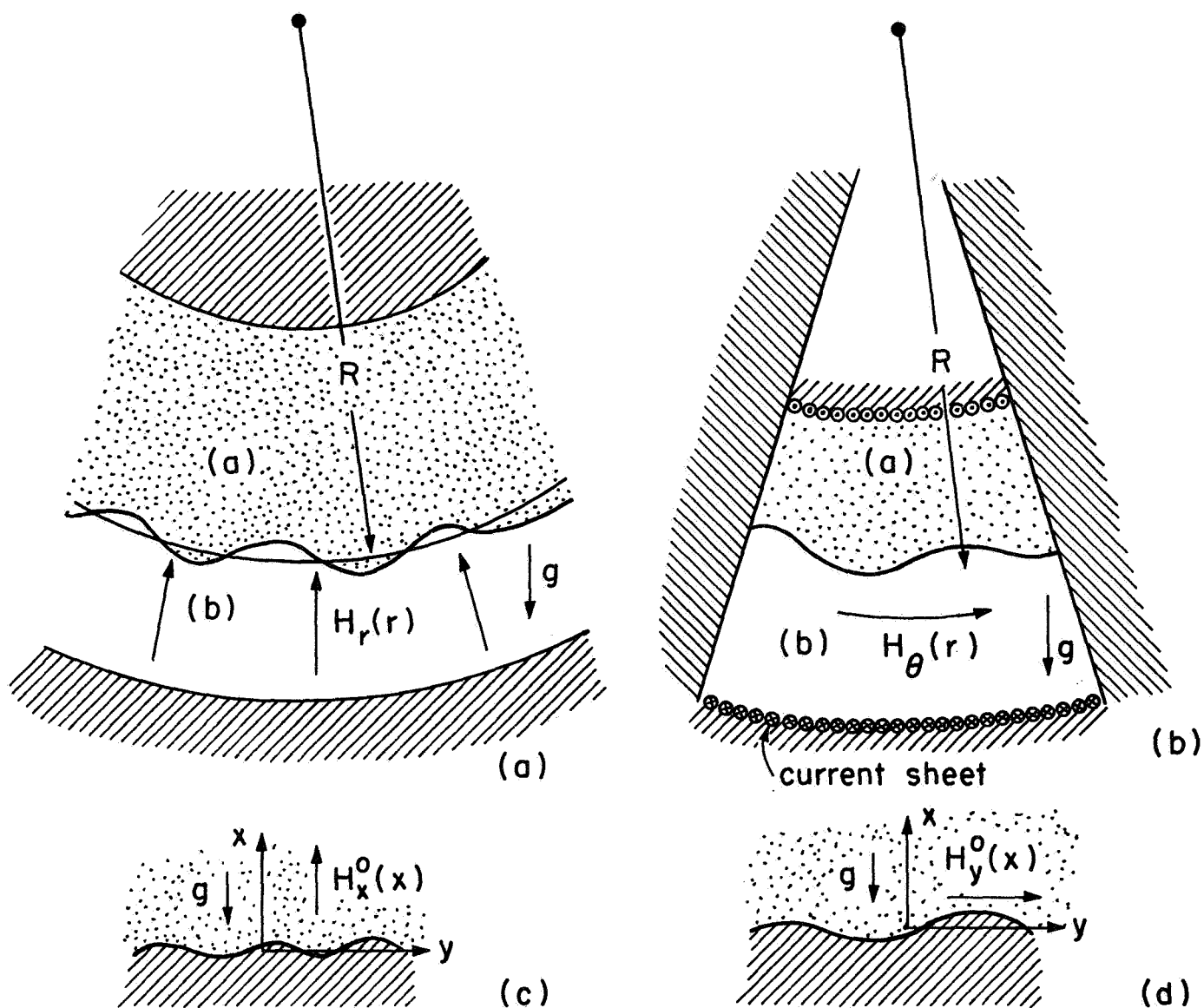


Fig. 3 Examples of nonuniform equilibrium fields: a) Field perpendicular to interface; b) Field tangential to interface; c) Quasi-one-dimensional model for (a); (d) Model for (b).

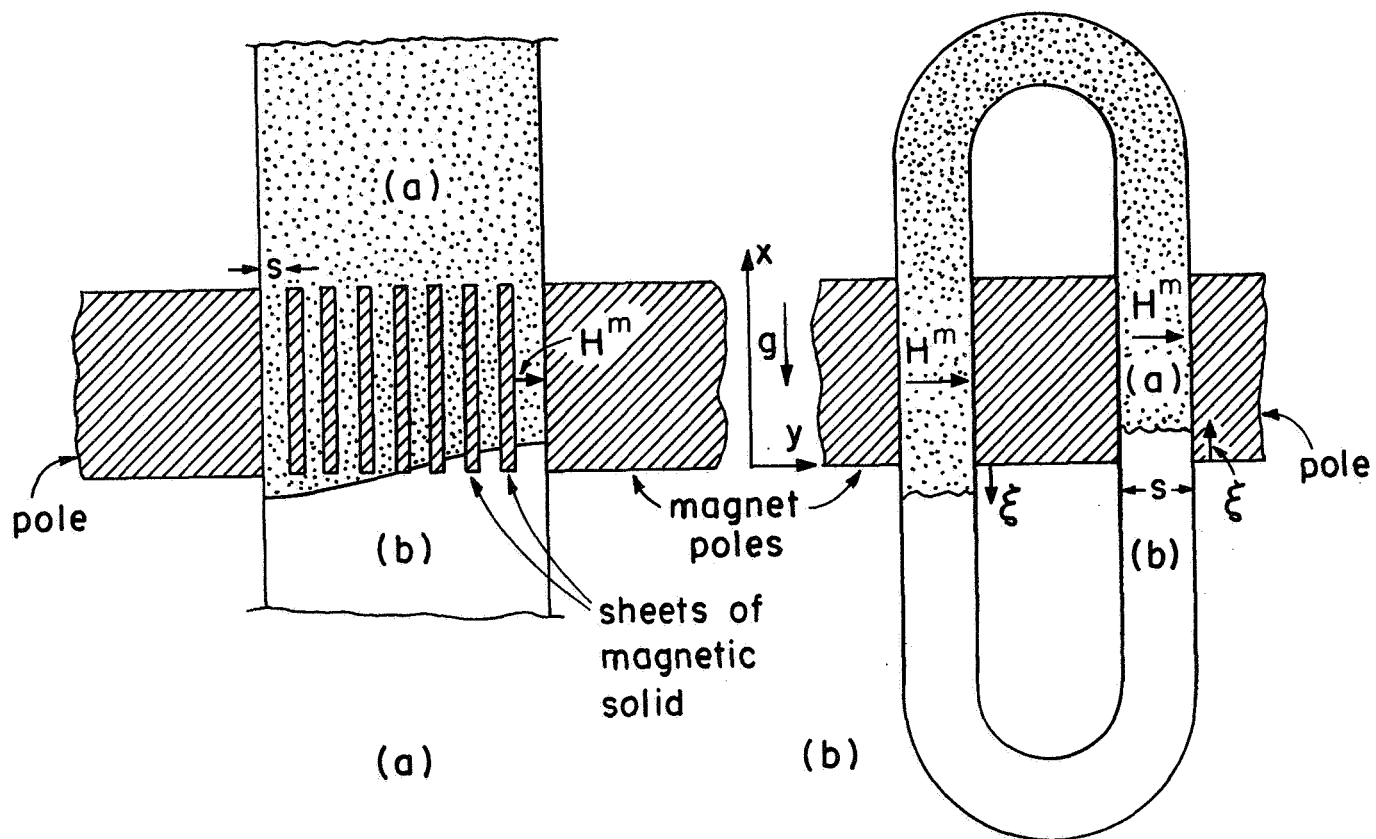


Fig. 4 a) Interface between fluids (a) and (b) interacts with field gradient concentrated in neighborhood of equilibrium interface.  
b) Pendulum model for (a).

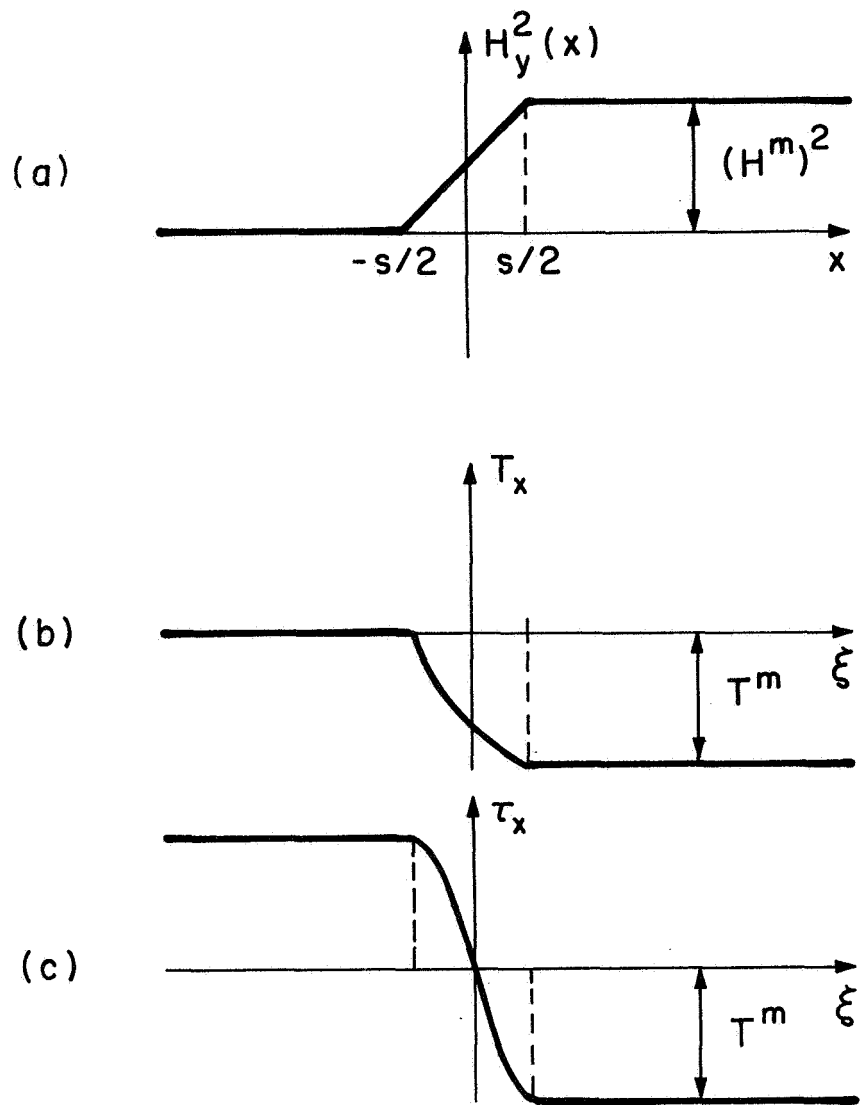


Fig. 5 a) Variation of imposed field intensity according to the quasi-one-dimensional model for concentrated field gradient configuration of Fig. 4.  
 b) Magnetic surface force density on right interface in Fig. 4(b).  
 c) Total magnetic force (per unit y-z area) on equivalent pendulum of Fig. 4(b).

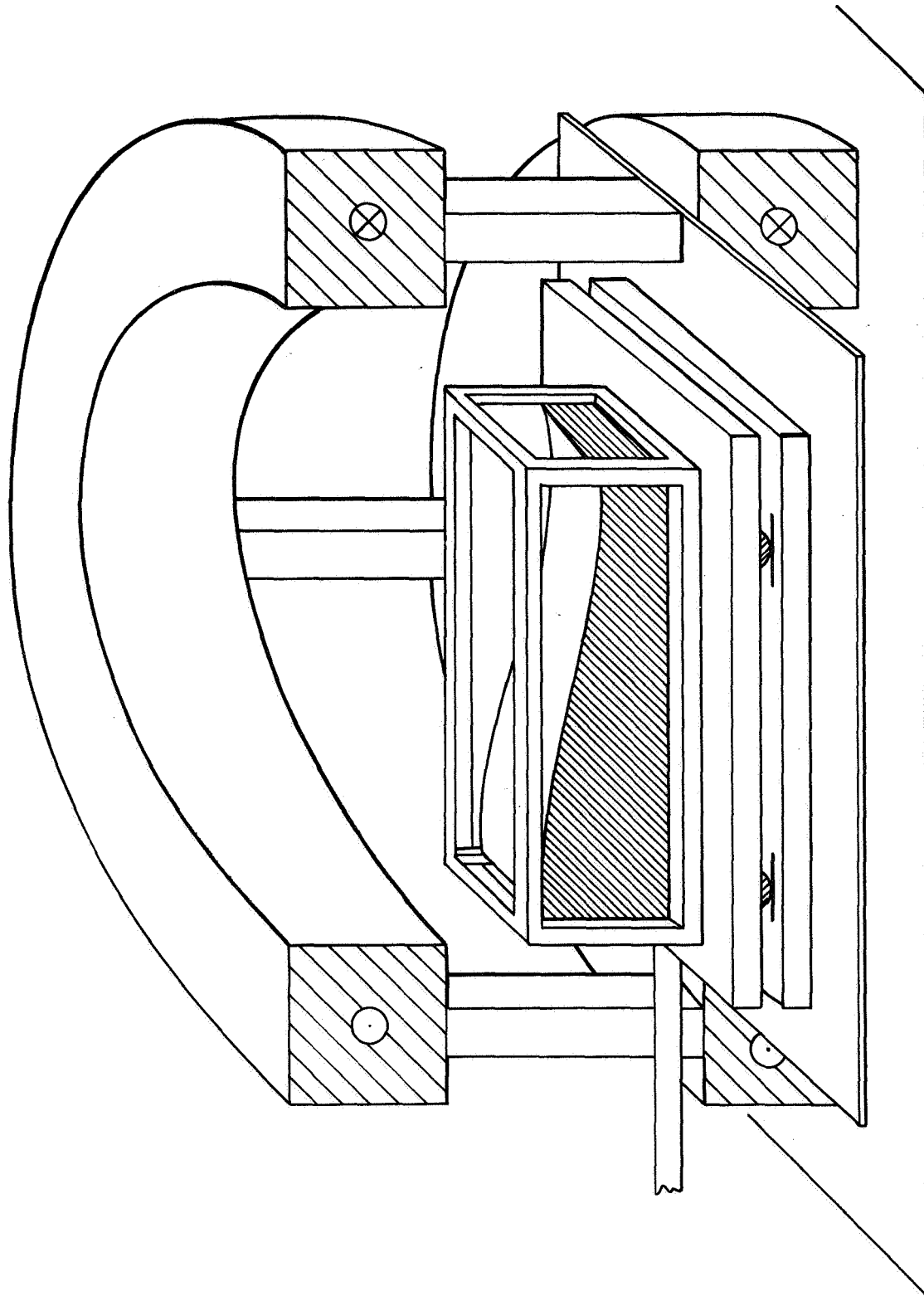
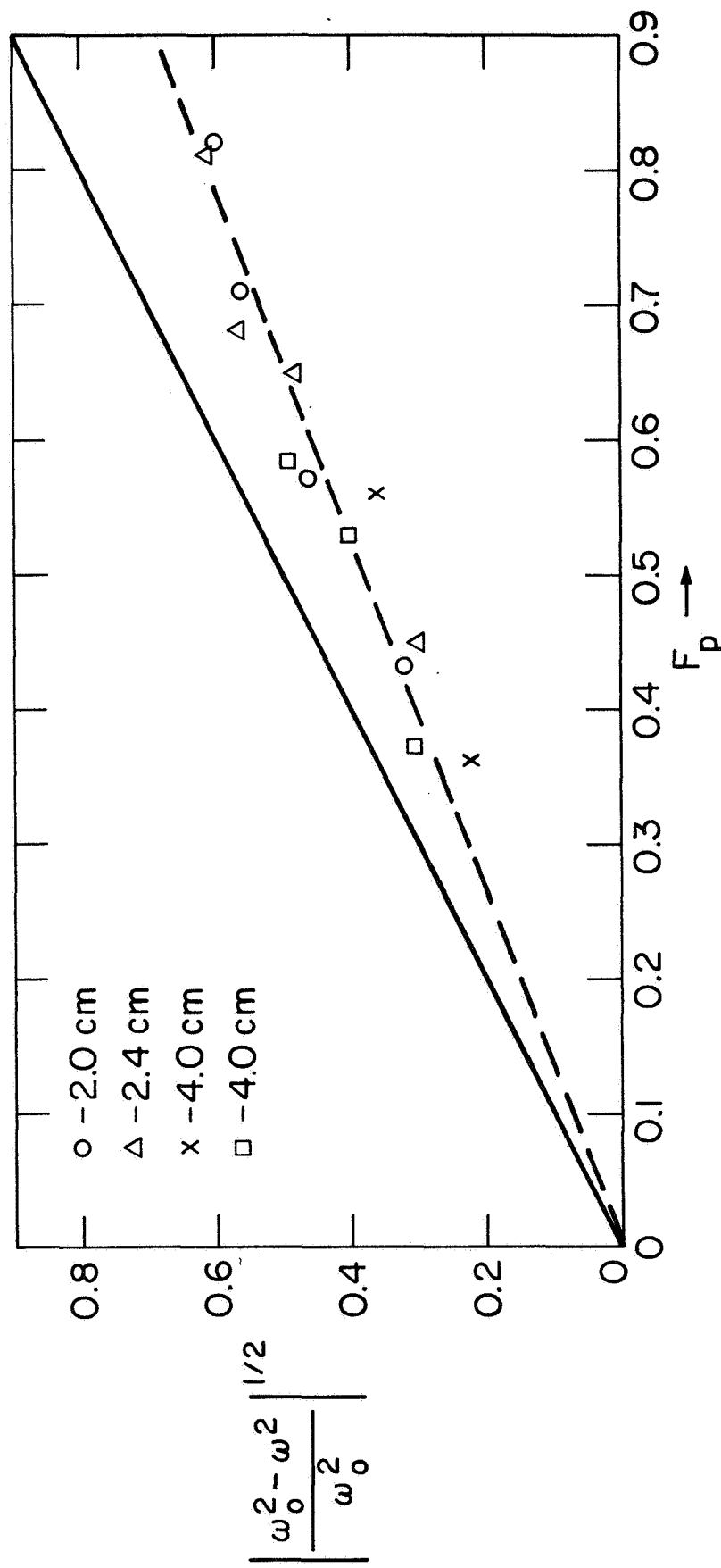


Fig. 6 a) Apparatus for measuring resonance frequencies with field imposed perpendicular to interface; vibrations of the tank in the horizontal plane drive the waves.



b) Relative frequency shift as a function of the parameter  $F_p$ , proportional to the applied field intensity. The frequency shifts downward as the applied field intensity is increased.

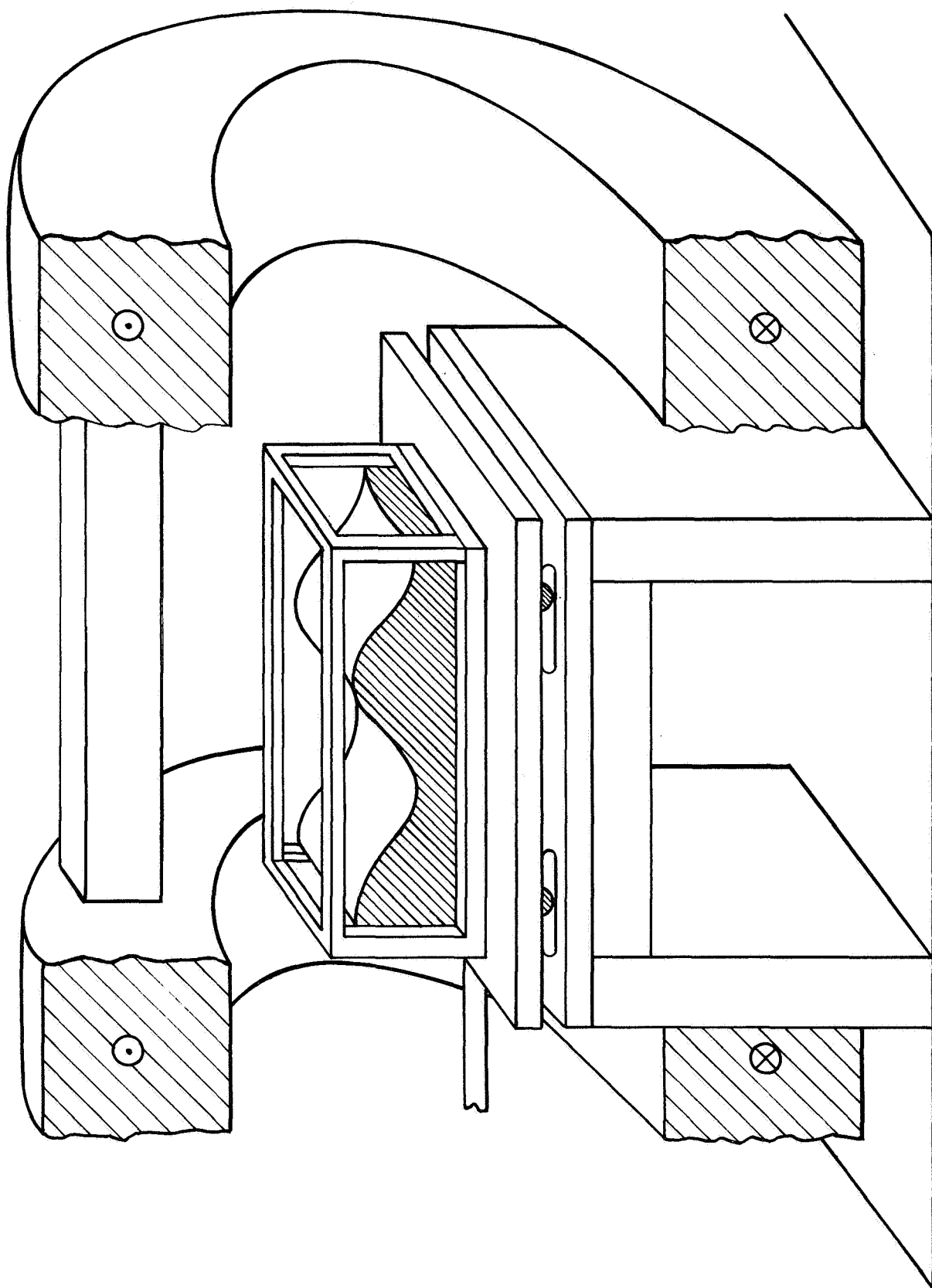
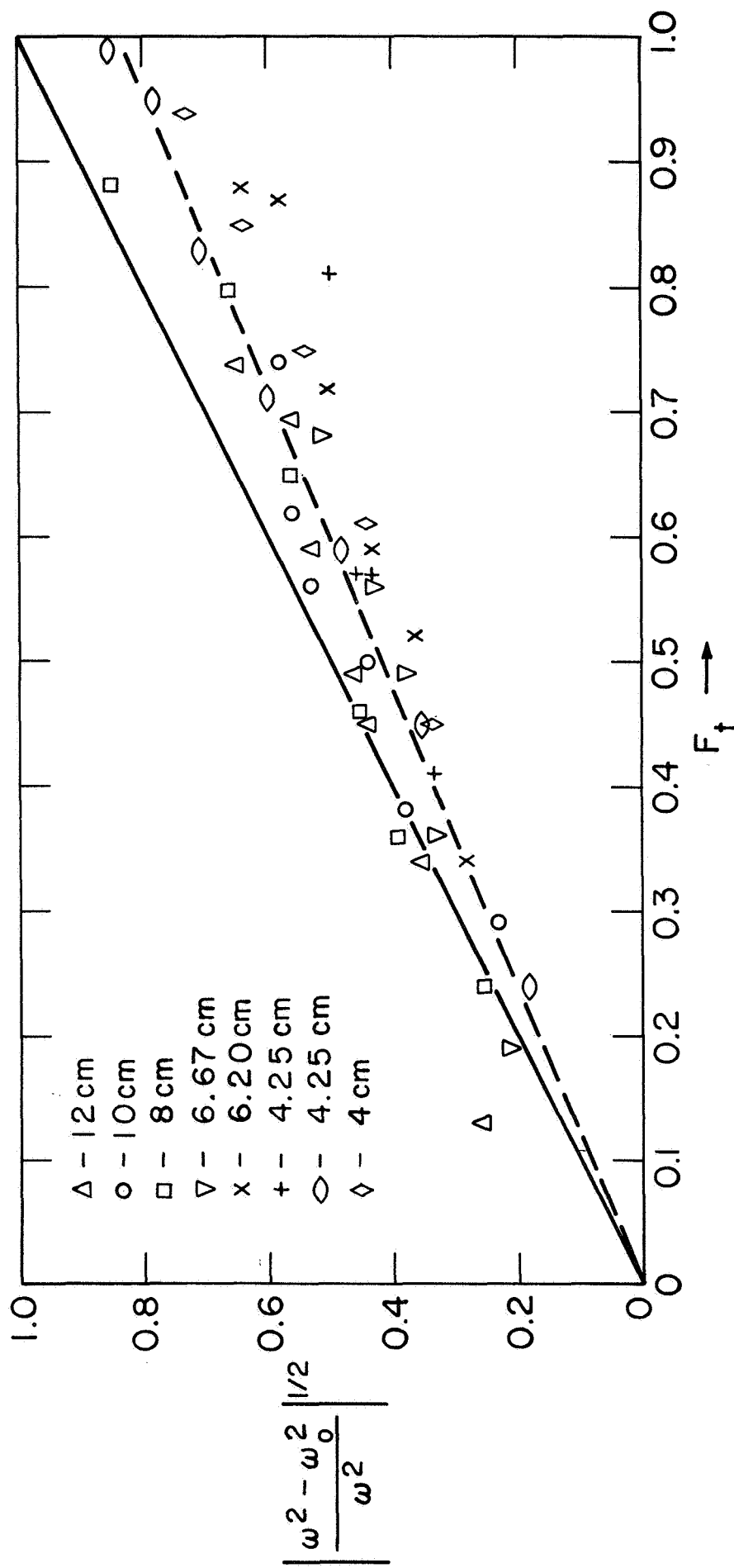


Fig. 7 a) Apparatus for measuring resonance frequencies in tangential field



b) Relative frequency shift as a function of  $F_t$ , a parameter proportional to the imposed magnetic field intensity.  $F_t$  is defined as the square root of the last term in Eq. (42) divided by  $\omega_0 \sqrt{\rho}$ .



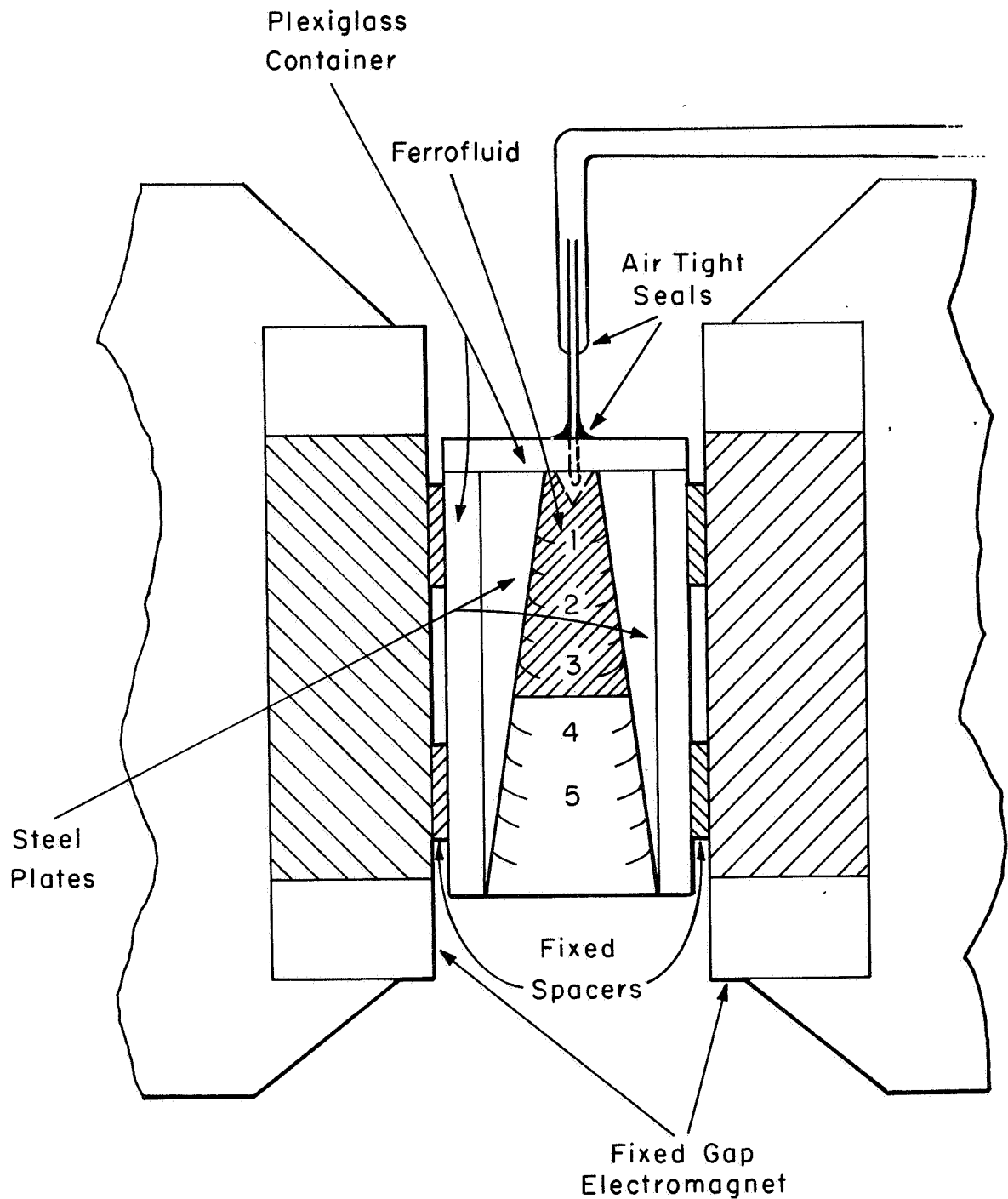
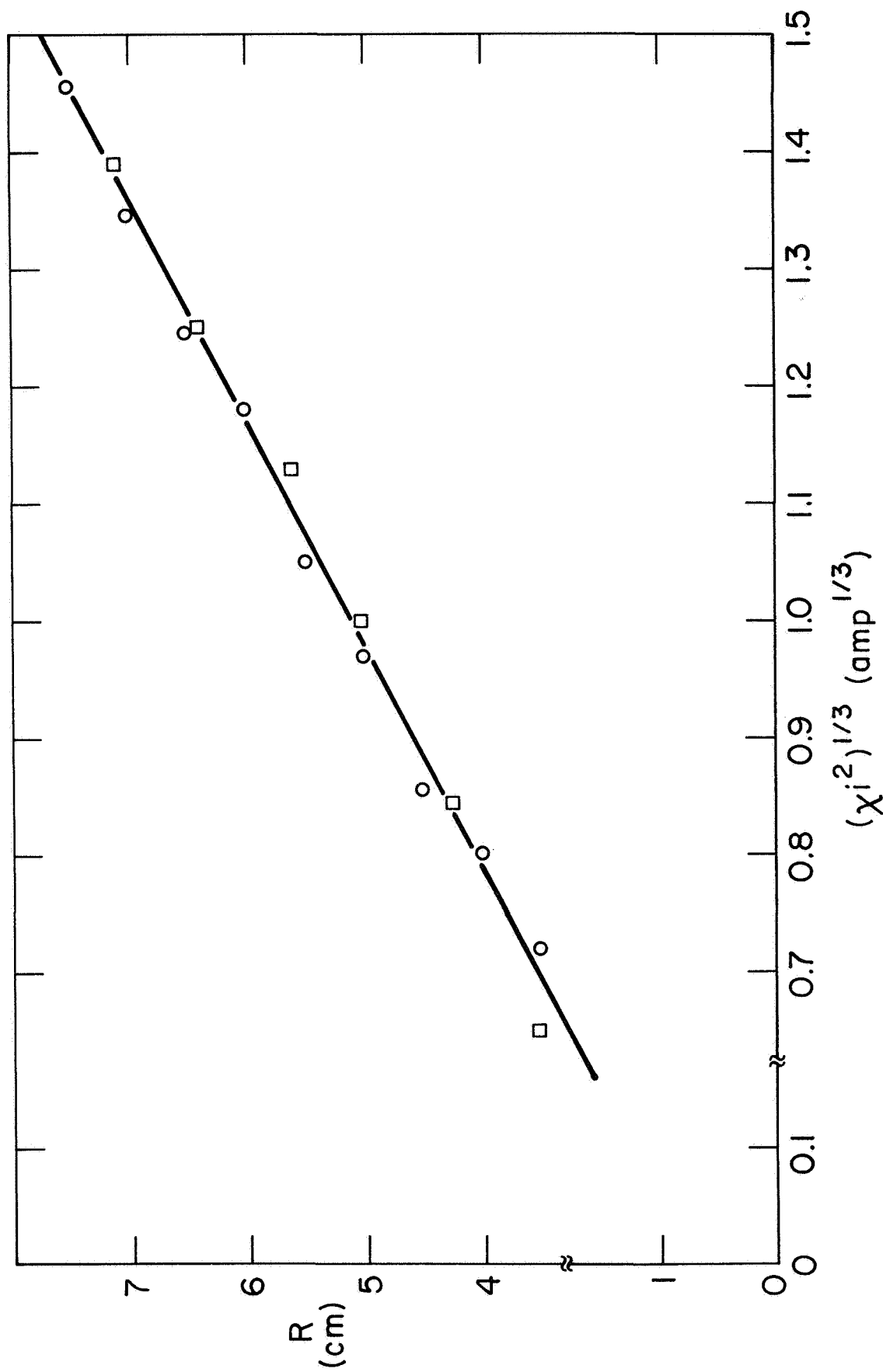


Fig. 8 a) Apparatus for measuring conditions for instability on interface in adverse gravitational acceleration. Magnetized steel plates provide the gradient in imposed field intensity required to stabilize the interface.



b) Conditions under which incipient instability is observed.  $R$  is the distance from the interface to the point at which the inner surfaces of the steel plates would converge if extended upward, while  $i$  is the magnet current. The solid curve is predicted by Eq. (57).